

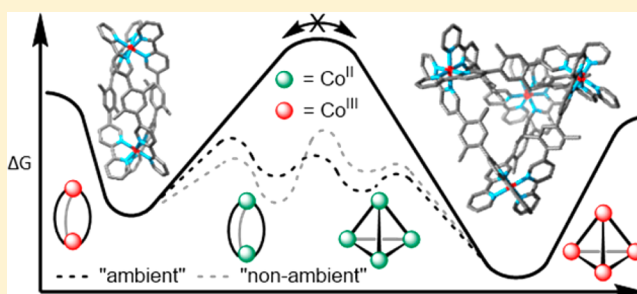
Orthogonal Selection and Fixing of Coordination Self-Assembly Pathways for Robust Metallo-organic Ensemble Construction

Michael J. Burke, Gary S. Nichol, and Paul J. Lusby*

EaStCHEM School of Chemistry, University of Edinburgh, Joseph Black Building, David Brewster Road, Edinburgh, Scotland EH9 3FJ, U.K.

S Supporting Information

ABSTRACT: Supramolecular construction strategies have overwhelmingly relied on the principles of thermodynamic control. While this approach has yielded an incredibly diverse and striking collection of ensembles, there are downsides, most obviously the necessity to trade-off reversibility against structural integrity. Herein we describe an alternative “assembly-followed-by-fixing” approach that possesses the high-yielding, atom-efficient advantages of reversible self-assembly reactions, yet gives structures that possess a covalent-like level of kinetic robustness. We have chosen to exemplify these principles in the preparation of a series of M_2L_3 helicates and M_4L_6 tetrahedra. While the rigidity of various bis(bidentate) ligands causes the larger species to be energetically preferred, we are able to freeze the self-assembly process under “non-ambient” conditions, to selectively give the disfavored M_2L_3 helicates. We also demonstrate “kinetic-stimuli” (redox and light)-induced switching between architectures, notably reconstituting the lower energy tetrahedra into highly distorted helicates.



INTRODUCTION

Discrete supramolecular constructs continue to provide notable interest because of their myriad applications from medicine¹ through catalysis² to storage and protection.³ The discovery of these functional properties has been enabled by straightforward, high-yielding synthetic methodology, which has permitted access to a wide and diverse set of architectures. The mainstay of these synthetic methods has been thermodynamically controlled self-assembly protocols,⁴ and in this regard certain metal–ligand interactions are ideally suited,⁵ providing an appropriate balance between strength—ensuring that closed systems are energetically favored over a wide range of concentrations—and reversibility, which allows the necessary exploration of the potential energy landscape. However, this method and the systems it produces are not without drawbacks. First, the thermodynamic selectivity for a particular species may sometimes be poor, as can be the case for square–triangle equilibria.⁶ While finely balanced equilibria are interesting from a fundamental supramolecular or system’s perspective, and can be readily exploited as adaptive chemical entities,⁷ the isolation of an individual component from a supramolecular product mixture can be highly challenging, if not impossible. Even with systems where a thermodynamic sink leads to a single product, the reversibility of metal–ligand interactions can still limit assembly integrity to rather specific “ambient” conditions, and this is despite the inherent kinetic stabilization that most metallosupramolecular species exhibit due to cooperative chelate effects.⁸

Chemical locking provides an ideal strategy to overcome the problems associated with weak interactions,⁹ allowing systems to be “fixed” at a given equilibrium position. Similar strategies are widespread for dynamic covalent chemistry (DCC), where reversible reactions are often made non-labile by changing conditions, by post-assembly modification, or through removal of a catalyst.¹⁰ While DCC has been used widely to give high-yielding access to complex yet often robust organic scaffolds, such as interlocked architectures¹¹ or cages,¹² more recently the interconversion between dynamic and non-dynamic states has been exploited to create molecular devices using orthogonal pairs of responsive covalent bonds.¹³

In the context of metallosupramolecular species, the most widely used strategy to create kinetically stable ensembles has been to exploit non-labile metal ions,¹⁴ most commonly second- and third-row d-block elements,¹⁵ which become dynamic only at elevated temperature. One of the earliest as well as most elegant and striking examples of this was Fujita’s isolation of a Pt catenane—particularly notable because this topologically non-trivial species appears thermodynamically non-favored under “standard” conditions.^{15a} The main problem, however, with using temperature as a “kinetic stimulus” is that it is non-selective with respect to the thermodynamics of any given system, because it additionally perturbs any equilibrium where $\Delta S \neq 0$. Also, the use of non-labile metal ions can lead to low yields or kinetically trapped

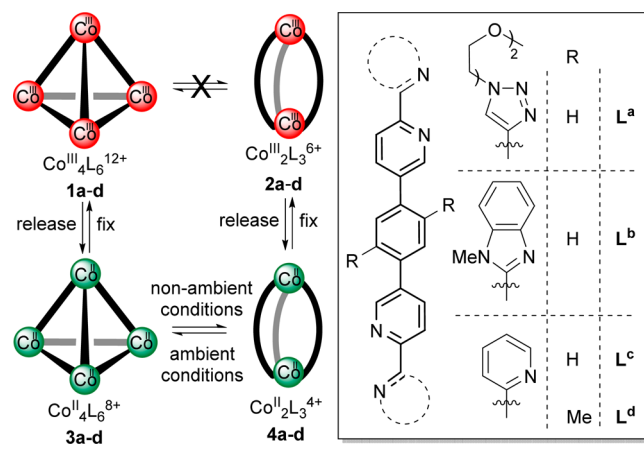
Received: May 25, 2016

Published: June 28, 2016

intermediates.^{1a,15e,16} The Fujita group have sought to overcome these issues through the application of solvochemical methods¹⁷ and light,¹⁸ which serve as “kinetic stimuli” to activate otherwise non-labile interactions. The use of light—which functions by switching the mechanism of Pt-substitution reactions¹⁸—is particularly notable because this kinetic activation is orthogonal to the thermodynamics of the system. Despite the elegance and benefits of this approach, this light-activated assembly procedure has not become widespread, having been limited (as far as we are aware) to the preparation of a metallocsupramolecular catenate,^{18a} a triangle,^{18b} and a single hexanuclear octagonal cage.

Recently, we targeted an oxidative deactivation strategy for accessing robust coordination assemblies.¹⁹ This method utilizes the substitutional non-lability of Co^{III} in comparison to Co^{II}.²⁰ This approach possesses many benefits, such as atom efficiency, high yields, and operational simplicity. At the same time, it produces robust products and exploits a cheap, abundant, less toxic first-row transition metal. Using a series of rigid bis(*N,N*-chelates) to demonstrate generality, we now develop this approach much further by showing that, in addition to the preferred tetrahedra, **1a–d**, we can also adapt the reaction to give the highly distorted helicates, **2a–d**, with complete selectivity (Scheme 1). These higher energy species,

Scheme 1. Selective Synthesis of Kinetically Robust Tetrahedra and Helicates Using an “Assembly-Followed-by-Fixing” Method



2a–d, would be otherwise difficult to isolate with a non-locked system.²¹ We also show that the system dynamics can be switched back “on” using both redox- and photoredox-based stimuli. These have been applied to interconvert different assemblies, most notably reconstituting tetrahedra into helicates, thus moving energetically uphill. Mechanisms that allow the potential energy landscape to be traversed using ratcheting inputs are important to fields such as molecular machines and motors.²²

RESULTS AND DISCUSSION

Pre-oxidation Co^{II} Equilibrium and Variable Oxidation Rate Studies. **1a** was previously obtained as a single species when cerium ammonium nitrate (CAN) was added dropwise to a 3:2 mol ratio of L^a and Co(ClO₄)₂·6H₂O in CH₃CN at room temperature.¹⁹ To determine whether the single fixed product is representative of the dynamic state, we decided to investigate the equilibrium between L^a and Co(ClO₄)₂·6H₂O in CD₃CN

using ¹H NMR spectroscopy (Figure 1). Interestingly, a solution at a concentration typical of the assembly-followed-

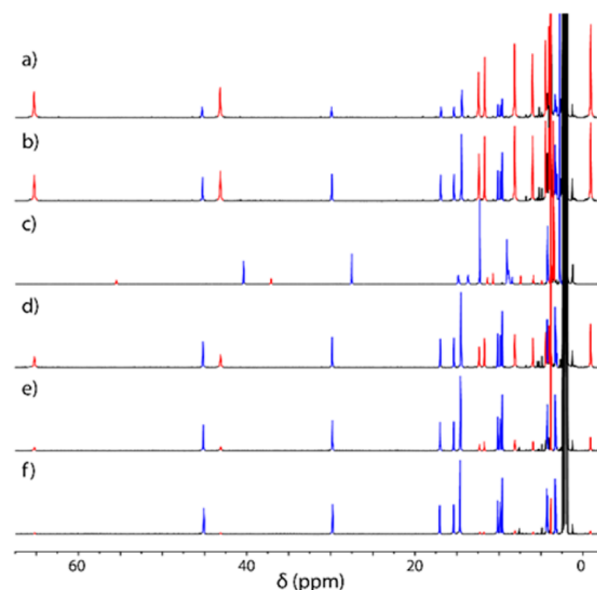
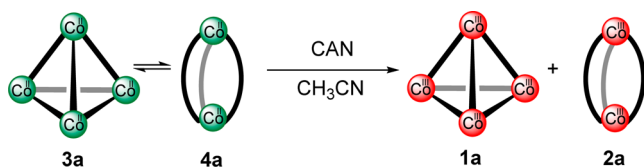


Figure 1. Partial ¹H NMR spectra (500 MHz, CD₃CN, 300 K unless stated) showing the equilibrium between **4a** (blue) and **3a** (red) as a function of [Co^{II}]_{total} and temperature: (a) 11.7 mM, (b) 5.84 mM, (c) 5.84 mM @ 343 K, (d) 2.92 mM, (e) 1.46 mM, and (f) 0.73 mM.

by-fixing method ([Co^{II}]_{total} = 11.7 mM) showed two paramagnetically shifted species (Figure 1a). This likely indicates a Co^{II} equilibrium between species of formulas (M₂L₃)_n^{7,21a,b,23} most obviously tetrahedron **3a** and helicate **4a**. This assignment is supported by a significant change in speciation following multiple dilutions of the stock L^a/Co^{II} solution (Figure 1b,d–f), which overall showed an increase in **4a** and a concomitant decrease in **3a** at lower concentrations. The rate of re-equilibration also occurred quickly; steady concentrations were reached within minutes of dilution, hence explaining why only **4a** was observed using the dilute conditions required for analysis by electrospray ionization mass spectrometry (ESI-MS). A similar thermodynamic switch was also observed at elevated temperature (Figure 1c), wherein the entropically favored **4a** (blue) increases at the expense of **3a** (red).

An implication of the Co^{II} equilibrium experiments was that dropwise addition of CAN to a mixture of **3a** and **4a** induces a helicate-to-tetrahedron constitutional rearrangement. We chose to further investigate this by varying the rate of oxidant addition with the ratio of **3a**:**4a** almost equal (55:45; [Co^{II}]_{total} = 5.56 mM; Table 1). This clearly confirmed that slow addition causes transformation into the larger species. It is interesting to note that the low [Co^{II}]_{total} toward the end of the fixing process should bias the equilibrium toward **4a**. Nonetheless, the slowest fixing reaction is completely selective for **1a**. An explanation for this could be the stronger preference of d⁶ Co^{III} for octahedral coordination geometry, wherein a small amount of Co^{III} “seeds” shift the equilibrium toward tetrahedral species. In contrast, when CAN is added rapidly to a vigorously stirred solution, the fixed product ratio (**1a**:**2a**) reflects the dynamic state (**3a**:**4a**) within the error of NMR integrations. Overall, it is interesting to compare the effects of slow and fast CAN addition: slow addition perturbs the bias of the system, whereas rapid

Table 1. Variation in Fixed Product Ratio 1a:2a as a Function of Rate of Oxidant Addition^{a,b}


| CAN total addition time | <5 s | 22 min ^c | 110 min ^c | 18 h 20 min ^c |
|-------------------------|-------|---------------------|----------------------|--------------------------|
| 1a:2a ratio | 51:49 | 87:13 | 95:5 | 99:1 |

^aReaction conditions: $[\text{Co}^{\text{II}}]_{\text{total}} = 5.56 \text{ mM}$, 1.5 equiv L^{a} , CH_3CN , 50 °C, 30 min, then CAN added at room temperature as a 11.7 mM CH_3CN solution. ^bInitial mole ratio of 3a:4a = 55:45. ^cCAN added at a constant rate using a syringe pump.

oxidation fixes the dynamics without changing the thermodynamic distribution.

Selective Co^{III} Helicate and Tetrahedron Synthesis.

Even though 4a is preferred only under dilute conditions, the capacity to fix the Co^{II} equilibrium without perturbation allowed 2a to be isolated as a single species. This was achieved by adding CAN rapidly to a vigorously stirred, dilute solution of L^{a} and $\text{Co}(\text{ClO}_4)_2 \cdot 6\text{H}_2\text{O}$ ($[\text{Co}^{\text{II}}]_{\text{total}} = 0.1 \text{ mM}$), from which 2a·6PF₆ was obtained in 93% yield. Even with ligands that show a greater thermodynamic preference for Co^{II} tetrahedra, as is the case with $\text{L}^{\text{b-d}}$ (see Supporting Information, section 3), the fixing reactions could be optimized to selectively give only Co^{III} helicates 2b–d (with isolated yields of 93%, 88%, and 64%, respectively). This is best exemplified with 2d. The ¹H NMR spectra of the Co^{II} equilibrium revealed a much stronger bias toward 3d (Figure S5); even under dilute conditions ($[\text{Co}^{\text{II}}]_{\text{total}} = 0.73 \text{ mM}$), the mole ratio of 3d:4d was 62:38 (cf. the mole ratio of 3a:4a, 4:96, at the same concentration). Nonetheless, oxidizing a very dilute solution of Co^{II} and L^{d} ($[\text{Co}^{\text{II}}]_{\text{total}} = 35 \mu\text{M}$) gave 2d as a single species. With the bipy ligands, $\text{L}^{\text{c,d}}$, we also observed that the Co^{II} states are much less dynamic, with equilibration of 3c:4c taking a week at room temperature (Figure S4). Long reaction times could be avoided, however, by adding the ligands to a very dilute solution of Co^{II} . When these reactions were oxidized immediately after ligand dissolution (ca. 1 h @ 50 °C), 2c,d were obtained exclusively. With these reactions it is likely that 4c,d are formed directly under kinetic control, thereby avoiding slow rearrangement from 3c,d. The Co^{III} helicates 2a–d have all been characterized by NMR and ESI-MS. In addition, the structures of 2c,d have been confirmed by X-ray crystallography (Figure 2b,d). The Co–N bond lengths are all what would be expected for Co^{III} (1.92–1.95 Å). Also, there is significant distortion to accommodate the closed structures; however, this appears to be manifested mainly in bending to the ligand frameworks, as both structures showed that Co^{III} adopts close to ideal octahedral geometry.²⁴

Co^{III} tetrahedra, 1b–d, were also selectively obtained starting from $\text{L}^{\text{b-d}}$. While the preceding Co^{II} equilibria all favor these larger species (see above), dropwise addition of the oxidant had a much less pronounced effect (see Supporting Information, section 4). Indeed, variable oxidation rate studies, analogous to those with L^{a} (e.g., Table 1), showed only a marginal increase in the proportion of 1c when CAN was added very slowly to a mixture of 3c and 4c (Table S1). This is consistent with the slower equilibration of bipy-based Co^{II} assemblies (see above). Nonetheless, the PF₆ salts of 1b–d were isolated as single compounds in yields of 78%, 77%, and 83%, respectively. As

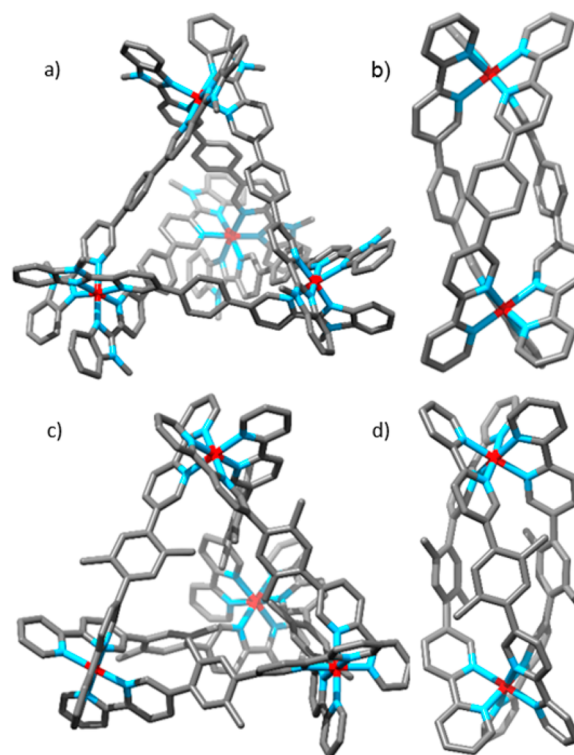


Figure 2. X-ray crystal structures of (a) 1b, (b) 2c, (c) 1d, and (d) 2d. Color code: carbon, gray; nitrogen, blue; cobalt, red. Hydrogen atoms, counteranions, and solvent omitted for clarity.

well as the relevant spectroscopic characterization, the structures of 1b and 1d have been confirmed by X-ray crystallography as homochiral *T*-symmetric architectures (Figure 2a,c).²⁵

Kinetic Robustness as a Function of Ligand Type. The Co^{III} coordination assemblies that feature the 2-(*N*-methylbenzimidazole)pyridyl, and even more so 2,2'-bipy chelates, show enhanced kinetic robustness in comparison to those formed from the pyridyl-triazole ligand L^{a} , as evidenced by the stability of the helicates 2a–d in solution (see Supporting Information, section 5). While 2a appears stable for weeks at room temperature in CD_3CN , when the sample is heated, slow yet complete rearrangement to 1a is observed by ¹H NMR spectroscopy, with this taking 1 week at 40 °C and then another week at 50 °C, followed by 2 days at 60 °C (Figure S9). This transformation also indicates that, as expected, 1a is energetically preferred in comparison to 2a, further confirming that the assembly-followed-by-fixing method is able to trap species that are thermodynamically disfavored. In contrast, 2c does not show any signs of change when heated for a week each at 40, 50, 60, and then 70 °C (2b shows intermediate stability, showing complete conversion to tetrahedron following 6 days at the 60 °C stage; Figures S10 and S11). These results indicate that the kinetic stability of 2a–c qualitatively matches the dynamics of the Co^{II} state with ligands $\text{L}^{\text{a-c}}$. A comparison of the bipy-based helicates (2c vs 2d) reveals that, as perhaps could be anticipated, the increased steric bulk marginally reduces the kinetic stability, with slight conversion to 1d observed after the same heating regime (Figure S12).

Kinetic-Stimuli-Induced Switching of Coordination Architectures. As none of the Co^{III} helicates 2a–d rearrange to their corresponding tetrahedra 1a–d at room temperature,

we concluded that this transformation could be readily used to probe the switching between locked and unlocked states. While metallosupramolecular transformations have become increasingly common,^{7,23a,d–j,26} these have overwhelmingly utilized stimuli that achieve switching by altering the thermodynamic preference of the system. In contrast, we sought to manipulate through a different mechanism—by selectively revealing a lower barrier between energy minima (Figure 3) rather than by

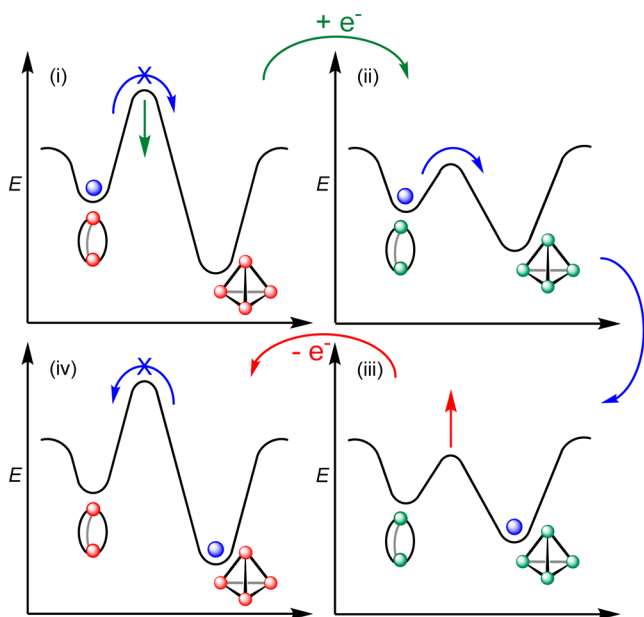
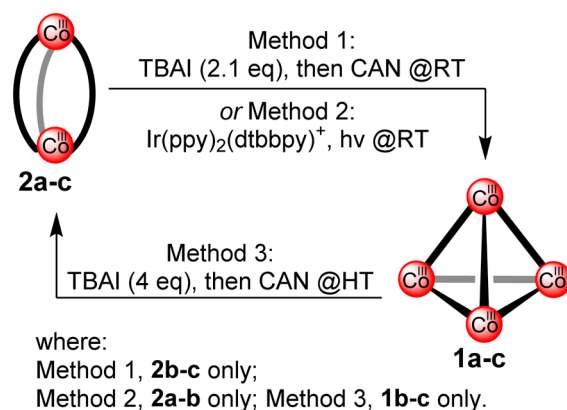


Figure 3. Energy profile diagrams showing a generic, kinetic-stimuli-induced helicate-to-tetrahedron transformation.

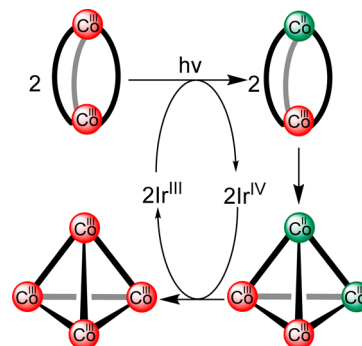
altering the relative depths of the energy wells on the potential energy surface. Initially focusing on the more robust helicates **2b,c**, we were pleased to observe that, when a slight excess of tetrabutylammonium iodide (TBAI) was added, the ¹H NMR spectra revealed the loss of the starting material resonances and the appearance of paramagnetically shifted signals (Figures S13 and S14), indicating the formation of Co^{II} complexes. In the case of **2c**, the predominant species formed was the metastable **4c** (Figure S14b), which over 5 days at room temperature was gradually replaced by **3c** (Figure S14c). Dropwise addition of CAN to the equilibrated Co^{II} samples gave exclusively **1b** and predominantly **1c**, respectively (Figures S13d and S14d). Starting far away from equilibrium, we can utilize stimuli that mainly affect the dynamics of ligand exchange to bring about this transformation selectively at ambient temperatures (Scheme 2, Method 1; Figure 3).

We have also explored the use of photoredox methods, which are currently enjoying a renaissance in organic synthetic applications,²⁷ for transforming the helicates into tetrahedral species. In this case we envisaged that a low steady-state concentration of Co^{II} species would facilitate rearrangement, and that the re-oxidation process would be achieved by closure of the photoredox catalytic loop (Scheme 2, Method 2; Scheme 3). In the case of both **2a** and **2b**, light irradiation in the presence of stoichiometric Ir(ppy)₂(dtbbpy)·PF₆ resulted in complete consumption of the helicate ¹H NMR signals and the appearance of **1a** and **1b** following 35 h and 4 days of irradiation using just a standard 42 W light bulb (Figures S17 and S19). In contrast, **2c** showed only very light change after 9

Scheme 2. “Kinetic-Stimuli-Induced” Assembly Interconversions



Scheme 3. Proposed Photoredox-Induced Assembly Conversion Mechanism



days of irradiation (Figure S21). This difference in photoredox reactivity is likely caused by the lower kinetic lability of the Co^{II} species with bipy ligands (see above). With **2a,b**, the lack of the same conversion in the absence of light (Figures S18 and S20) and the quenching of the Ir(ppy)₂(dtbbpy)⁺ luminescence in the presence of the Co^{III} species both support a photoredox mechanism that involves single electron transfer from the excited state of Ir^{III} to Co^{III}. The relatively slow rate of these rearrangement reactions, even with stoichiometric Ir^{III} complex, is likely caused by a bimolecular mechanism that involves two mixed-valence Co^{III}–Co^{II} species (Scheme 3) and the corresponding low steady-state concentration of this species generated through the photoredox method.

The limitation of transforming one metallosupramolecular entity into another solely utilizing a stimulus that affects the thermodynamics of the system is that it is only possible to move energetically downhill. Thus, we were keen to demonstrate that it would also be possible to reconstitute a tetrahedron into a helicate, taking advantage of the ability to kinetically trap the system in a high-energy state. Pleasingly, we have been able to successfully reconstitute both **1b** and **1c**—the more robust tetrahedra—into their corresponding, higher energy helicates, **2b** and **2c**. This was achieved by first unlocking with a stoichiometric amount of TBAI reductant, and then by rapidly re-locking the system via the rapid addition of CAN at elevated temperature (343 K) to trap the entropically smaller assembly. With this method we exclusively or overwhelmingly obtain the higher energy species, **2b** and **2c** (Scheme 2, Method 3; Figures S15 and S16).

CONCLUSIONS

The assembly-followed-by-fixing method we have exemplified here allows high-yielding access to structures not thermodynamically favored under “ambient” conditions. Furthermore, the wide and varied range of architectures that have previously been obtained using Co^{II} and different bridged bidentate ligands,^{2,3d,e,j} and also the potential to explore more extreme “non-ambient” conditions (pressure, larger temperature ranges, etc.), point to a very wide range of assemblies that are potentially attainable. It could be anticipated that these, like the ones presented here, will possess a kinetic stability not usually associated with many metal–organic ensembles. While there are other approaches to creating robust cage-type systems, notably the formation of fully covalent (organic) architectures,^{12,28} these systems generally lack the in-built mechanism whereby the structure can be (selectively) made labile using a simple redox (or photoredox)-based stimuli. These features, along with the recent report of hypoxic activation of Co^{III} prodrugs,²⁹ make water-soluble analogues of the capsules reported here²² prime candidates for biological testing. Such investigations using these and related systems are currently underway in our laboratory.

EXPERIMENTAL METHODS

General. All reagents were purchased from commercial sources and used without further purification. All ¹H and ¹³C NMR spectra were recorded on either Bruker AV400, AV500, PRO500, or AV600 instruments at a constant temperature of 300 K unless stated otherwise. Chemical shifts are reported in parts per million from low to high field, referenced against values for the residual solvent peaks. Coupling constants (*J*) are reported as observed in Hz. Standard abbreviations indicating multiplicity were used as follows: m = multiplet, t = triplet, d = doublet, s = singlet, br(s/d) = broad (singlet/doublet etc.), appt = apparent triplet, etc. Mass spectrometry (ESI-MS) of all helicate and tetrahedron complexes was carried out using a Waters SYNAPT G2 instrument. The synthesis of L^a and 1a-12PF₆ has been previously reported.¹⁹

Syntheses. **1b-12PF₆.** To a suspension of L^b (0.0300 g, 60.9 μmol) in degassed acetonitrile (5.0 mL) was added cobalt(II) perchlorate hexahydrate (0.0149 g, 40.7 μmol), which after further degassing was heated at 50 °C for 1 h under an atmosphere of N₂. Once this mixture cooled to room temperature, cerium(IV) ammonium nitrate (0.0338 g, 61.6 μmol) in acetonitrile (5.4 mL) was added using a syringe pump at a rate of 25 μL/min. Once addition was complete, the precipitate was filtered onto Celite, washed with acetonitrile, and then eluted with water–acetonitrile (2:1, 15.0 mL). The addition of ammonium hexafluorophosphate (0.797 g, 4.89 mmol) to the solution resulted in the formation of a precipitate, which was filtered onto Celite, washed with water, and then eluted in acetonitrile before the solvent was removed under vacuum to give the title compound as a red solid. Yield = 0.0389 g (78%). ¹H NMR (500 MHz, CD₃CN): δ 8.88 (d, *J* = 8.7 Hz, 12H, *m*-pyridyl-*H*), 8.81 (dd, *J* = 8.6, 1.8 Hz, 12H, *p*-pyridyl-*H*), 7.96 (d, *J* = 8.6 Hz, 12H, benzimidazole-*H*), 7.61 (ddd, *J* = 8.4, 7.3, 0.9 Hz, 12H, benzimidazole-*H*), 7.58 (d, *J* = 1.6 Hz, 12H, *o*-pyridyl-*H*), 7.49 (s, 24H, C₆H₄), 7.13 (ddd, *J* = 8.4, 7.2, 1.0 Hz, 12H, benzimidazole-*H*), 5.35 (d, *J* = 8.6 Hz, 12H, benzimidazole-*H*), 4.55 (s, 36H, N–CH₃). ¹³C NMR (126 MHz, CD₃CN): δ 151.6, 150.9, 146.1, 142.0, 141.5, 139.8, 138.6, 135.4, 129.1, 129.0, 128.7, 128.2, 115.4, 115.1, 35.2. ¹H DOSY NMR (500 MHz, CD₃CN): *D* = 4.73 × 10^{−6} cm² s^{−1}; calculated hydrodynamic radius = 12.5 Å. ESI-MS (*m/z*): 1087 (+4), 841 (+5), 676 (+6), 559 (+7), 471 (+8), 402 (+9) (see Supporting Information, section 8, for expansions of each charge state and comparison with calculated isotopic distributions). Red crystals of 1b-12PF₆ suitable for X-ray diffraction studies were grown by slow diffusion of diisopropyl ether into a saturated acetonitrile solution. X-ray analysis (CCDC 1425917) is detailed in Supporting Information, section 9.

1c-12PF₆. Following a method similar to that reported for 1b-12PF₆ initially by adding cobalt(II) perchlorate hexahydrate (0.0136 g, 37.2 μmol) to a suspension of L^c (0.0215 g, 55.6 μmol) in acetonitrile (3.0 mL), the title compound was isolated as a yellow solid. Yield = 0.0307 g (77%). ¹H NMR (500 MHz, CD₃CN): δ 8.93 (d, *J* = 8.6 Hz, 12H, *endo-m*-pyridyl-*H*), 8.87 (dd, *J* = 8.5, 1.9 Hz, 12H, *endo-p*-pyridyl-*H*), 8.82 (dd, *J* = 8.2, 1.5 Hz, 12H, *exo-m*-pyridyl-*H*), 8.58–8.50 (m, 12H, *exo-p*-pyridyl-*H*), 7.82 (ddd, *J* = 7.6, 5.9, 1.4 Hz, 12H, *exo-m*-pyridyl-*H*), 7.46 (s, 24H, C₆H₄), 7.35 (d, *J* = 6.0 Hz, 12H, *exo-o*-pyridyl-*H*), 7.31 (d, *J* = 2.0 Hz, 12H, *endo-o*-pyridyl-*H*). ¹³C NMR (126 MHz, CD₃CN): δ 155.2, 154.7, 151.7, 148.0, 144.0, 141.3, 140.7, 134.3, 131.8, 128.0, 127.7, 126.9. ¹H DOSY NMR (500 MHz, CD₃CN): *D* = 4.90 × 10^{−6} cm² s^{−1}; calculated hydrodynamic radius = 12.1 Å. ESI-MS (*m/z*): 928 (+4), 713 (+5), 570 (+6), 468 (+7), 392 (+8), 284 (+10), 245 (+11) (see Supporting Information, section 8, for expansions of each charge state and comparison with calculated isotopic distributions).

1d-12PF₆. Following a method similar to that reported for 1b-12PF₆ initially by adding cobalt(II) perchlorate hexahydrate (0.0132 g, 36.1 μmol) to a suspension of L^d (0.0223 g, 53.8 μmol) in acetonitrile (2.9 mL), the title compound was isolated as a yellow solid. Yield = 0.0332 g (83%). ¹H NMR (500 MHz, CD₃CN): δ 8.74–8.70 (m, 24H, *exo-m*-pyridyl-*H* and *endo-m*-pyridyl-*H*), 8.54–8.49 (m, 12H, *exo-p*-pyridyl-*H*), 8.35 (dd, *J* = 8.4, 1.7 Hz, 12H, *endo-p*-pyridyl-*H*), 7.78 (ddd, *J* = 7.5, 5.9, 1.4 Hz, 12H, *exo-m*-pyridyl-*H*), 7.49 (d, *J* = 1.7 Hz, 12H, *endo-o*-pyridyl-*H*), 7.26 (dd, *J* = 6.0, 1.2 Hz, 12H, *exo-o*-pyridyl-*H*), 6.97 (s, 12H, C₆H₂(CH₃)₂), 1.88 (s, 36H, C₆H₂(CH₃)₂). ¹³C NMR (126 MHz, CD₃CN): δ 156.3, 155.8, 152.6, 150.5, 146.0, 145.2, 144.8, 136.5, 134.6, 133.1, 132.9, 128.7, 128.2, 20.3. ¹H DOSY NMR (500 MHz, CD₃CN): *D* = 4.75 × 10^{−6} cm² s^{−1}; calculated hydrodynamic radius = 12.4 Å. ESI-MS (*m/z*): 1341 (+3), 970 (+4), 747 (+5), 598 (+6), 350 (+9), 301 (+10), 260 (+11) (see Supporting Information, section 8, for expansions of each charge state and comparison with calculated isotopic distributions). Yellow crystals of 1d-12PF₆ suitable for X-ray diffraction studies were grown by slow diffusion of diisopropyl ether into a saturated acetonitrile solution. X-ray analysis (CCDC 1425919) is detailed in Supporting Information, section 9.

2a-6PF₆. L^a (0.0450 g, 78.9 μmol) was added to cobalt(II) perchlorate hexahydrate (0.0192 g, 52.5 μmol) in acetonitrile (500 mL), which was then heated for 1 h to ensure complete dissolution of the ligand. Once the mixture cooled to room temperature, cerium(IV) ammonium nitrate (0.0585 g, 106.7 μmol) was added, and the forming precipitate was stirred for 0.5 h. The precipitate was then filtered onto Celite, washed with acetonitrile, and eluted with water–acetonitrile (2:1, 40 mL). The addition of ammonium hexafluorophosphate (1.03 g, 6.30 mmol) to the solution resulted in the formation of a precipitate, which was filtered onto Celite, washed with water, and then dissolved in acetonitrile before the solvent was removed under vacuum to give the title compound as an orange solid. Yield = 0.0659 g (93%). ¹H NMR (500 MHz, CD₃CN): δ 9.11 (s, 6H, triazole-*H*), 8.78 (d, *J* = 8.2 Hz, 6H, *p*-pyridyl-*H*), 8.55 (d, *J* = 8.2 Hz, 6H, *m*-pyridyl-*H*), 7.34 (s, 12H, C₆H₄), 6.71 (s, 6H, *o*-pyridyl-*H*), 4.83–4.69 (m, 12H, *peg-H*), 3.93 (t, *J* = 4.8 Hz, 12H, *peg-H*), 3.67–3.59 (m, 12H, *peg-H*), 3.52–3.46 (m, 12H, *peg-H*), 3.30 (s, 18H, *pegOCH₃*). ¹³C NMR (126 MHz, CD₃CN): δ 150.1, 150.0, 148.7, 142.8, 141.9, 136.6, 129.7, 129.4, 127.4, 72.4, 71.0, 68.9, 59.0, 55.2. ¹H DOSY NMR (500 MHz, CD₃CN): *D* = 5.94 × 10^{−6} cm² s^{−1}; calculated hydrodynamic radius = 10.0 Å. ESI-MS (*m/z*): 1204 (+2), 754 (+3), 529 (+4), 394 (+5) (see Supporting Information, section 8, for expansions of each charge state and comparison with calculated isotopic distributions).

2b-6PF₆. Following a method similar to that reported for 2a-6PF₆ starting with L^b (0.0543 g, 110 μmol) and cobalt(II) perchlorate hexahydrate (0.0269 g, 73.5 μmol) in acetonitrile (950 mL), the title compound was isolated as a red solid. Yield = 0.0421 g (93%). ¹H NMR (500 MHz, CD₃CN): δ 8.94–8.89 (m, 12H, *p*-pyridyl-*H* and *m*-pyridyl-*H*), 8.03 (d, *J* = 8.6 Hz, 6H, benzimidazole-*H*), 7.69 (appt, 6H, benzimidazole-*H*), 7.39 (s, 12H, C₆H₄), 7.21 (appt, 6H, benzimidazole-*H*), 6.49 (br s, 6H, *o*-pyridyl-*H*), 5.41 (d, *J* = 8.6 Hz, 6H, benzimidazole-*H*), 4.60 (s, 18H, N–CH₃). ¹³C NMR (126 MHz, CD₃CN): δ 151.3, 151.1, 148.0, 142.1, 141.7, 140.0, 138.3, 135.9,

129.8, 129.3, 129.1, 128.8, 115.4, 115.4, 35.2. ^1H DOSY NMR (500 MHz, CD_3CN): $D = 6.41 \times 10^{-6} \text{ cm}^2 \text{ s}^{-1}$; calculated hydrodynamic radius = 9.2 Å. ESI-MS (m/z): 676 (+3), 471 (+4), 348 (+5), 266 (+6) (see Supporting Information, section 8, for expansions of each charge state and comparison with calculated isotopic distributions).

2c-6PF₆. Following a method similar to that reported for **2a-6PF₆** starting with **L^c** (0.0419 g, 108 μmol) and cobalt(II) perchlorate hexahydrate (0.0265 g, 72.4 μmol) in acetonitrile (1 L), the title compound was isolated as a yellow solid. Yield = 0.0639 g (82%). ^1H NMR (500 MHz, CD_3CN): δ 8.90–8.86 (m, 12H, *endo-p*-pyridyl-*H* and *endo-m*-pyridyl-*H*), 8.82 (dd, $J = 8.1, 1.1$ Hz, 6H, *exo-m*-pyridyl-*H*), 8.64–8.57 (m, 6H, *exo-p*-pyridyl-*H*), 7.90 (ddd, $J = 7.6, 6.0, 1.4$ Hz, 6H, *exo-m*-pyridyl-*H*), 7.35 (s, 12H, C_6H_4), 7.31 (dd, $J = 6.0, 0.7$ Hz, 6H, *exo-o*-pyridyl-*H*), 6.34 (br s, 6H, *endo-o*-pyridyl-*H*). ^{13}C NMR (126 MHz, CD_3CN): δ 156.1, 156.1, 151.7, 148.6, 144.1, 142.0, 141.0, 135.0, 132.0, 128.4, 128.2, 127.9. ^1H DOSY NMR (500 MHz, CD_3CN): $D = 6.48 \times 10^{-6} \text{ cm}^2 \text{ s}^{-1}$; calculated hydrodynamic radius = 9.2 Å. ESI-MS (m/z): 570 (+3), 391 (+4), 284 (+5), 212 (+6) (see Supporting Information, section 8, for expansions of each charge state and comparison with calculated isotopic distributions). Yellow crystals of **2c-6BF₄** (prepared by adding NaBF_4 at ion metathesis stage) suitable for X-ray diffraction studies were grown by slow diffusion of diisopropyl ether into a saturated acetonitrile solution. X-ray analysis (CCDC 1425918) is detailed in Supporting Information, section 9.

2d-6PF₆. Following a method similar to that reported for **2a-6PF₆** starting with **L^d** (0.0109 g, 26.3 μmol) and cobalt(II) perchlorate hexahydrate (0.0064 g, 17.5 μmol) in acetonitrile (500 mL), the title compound was isolated as an orange solid. Yield = 0.0063 g (64%). ^1H NMR (500 MHz, CD_3CN): δ 8.88 (d, $J = 8.5$ Hz, 6H, *endo-m*-pyridyl-*H*), 8.81 (dd, $J = 8.1, 1.5$ Hz, 6H, *exo-m*-pyridyl-*H*), 8.78 (dd, $J = 8.4, 1.8$ Hz, 6H, *endo-p*-pyridyl-*H*), 8.65–8.55 (m, 6H, *exo-p*-pyridyl-*H*), 7.89 (ddd, $J = 7.7, 6.0, 1.5$ Hz, 6H, *exo-m*-pyridyl-*H*), 7.23 (s, 6H, $\text{C}_6\text{H}_2(\text{CH}_3)_2$), 7.10 (dd, $J = 6.1, 1.3$ Hz, 6H, *exo-o*-pyridyl-*H*), 6.81 (d, $J = 1.9$ Hz, 6H, *endo-o*-pyridyl-*H*), 1.74 (s, 18H, $\text{C}_6\text{H}_2(\text{CH}_3)_2$). ^{13}C NMR (126 MHz, CD_3CN): δ 156.8, 156.3, 152.9, 149.6, 145.4, 144.2, 144.1, 135.4, 135.3, 133.4, 129.0, 129.0, 19.4. ^1H DOSY NMR (500 MHz, CD_3CN): $D = 6.33 \times 10^{-6} \text{ cm}^2 \text{ s}^{-1}$; calculated hydrodynamic radius = 9.3 Å. ESI-MS (m/z): 970 (+2), 598 (+3), 412 (+4), 301 (+5), 226 (+6) (see Supporting Information, section 8, for expansions of each charge state and comparison with calculated isotopic distributions). Yellow crystals of **2d-6BF₄** (prepared by adding NaBF_4 at ion metathesis stage) suitable for X-ray diffraction studies were grown by slow diffusion of diisopropyl ether into a saturated acetonitrile solution. X-ray analysis (CCDC 1429784) is detailed in Supporting Information, section 9.

■ ASSOCIATED CONTENT

Supporting Information

The Supporting Information is available free of charge on the ACS Publications website at DOI: 10.1021/jacs.6b05364.

X-ray crystallographic data for **1b-12PF₆** (CIF)

X-ray crystallographic data for **1d-12PF₆** (CIF)

X-ray crystallographic data for **2c-6BF₄** (CIF)

X-ray crystallographic data for **2d-6BF₄** (CIF)

Synthetic procedures and characterization of **L^{b-d}**; ^1H and ^{13}C NMR spectra of all new compounds; MS of all coordination assemblies; Co^{II} equilibrium experiments; variable oxidation rate studies; helicate stability experiments; redox and photoredox switching protocols; and X-ray crystallographic details (PDF)

■ AUTHOR INFORMATION

Corresponding Author

*paul.lusby@ed.ac.uk

Notes

The authors declare no competing financial interest.

Crystallographic data have been deposited with the Cambridge Crystallographic Data Centre as entries CCDC 1425917 (**1b-12PF₆**), 1425919 (**1d-12PF₆**), 1425918 (**2c-6BF₄**), and 1429784 (**2d-6BF₄**).

■ ACKNOWLEDGMENTS

This work was supported by the UK Engineering and Physical Sciences Research Council (EPSRC). We thank Dr. Euan R. Kay (University of St. Andrews) for useful discussions.

■ REFERENCES

- (1) (a) Pascu, G. I.; Hotze, A. C. G.; Sanchez-Cano, C.; Kariuki, B. M.; Hannon, M. J. *Angew. Chem., Int. Ed.* **2007**, *46*, 4374. (b) Therrien, B.; Suess-Fink, G.; Govindaswamy, P.; Renfrew, A. K.; Dyson, P. J. *Angew. Chem., Int. Ed.* **2008**, *47*, 3773. (c) Faulkner, A. D.; Kaner, R. A.; Abdallah, Q. M. A.; Clarkson, G.; Fox, D. J.; Gurnani, P.; Howson, S. E.; Phillips, R. M.; Roper, D. I.; Simpson, D. H.; Scott, P. *Nat. Chem.* **2014**, *6*, 797. (d) Grishagin, I. V.; Pollock, J. B.; Kushal, S.; Cook, T. R.; Stang, P. J.; Olenyuk, B. Z. *Proc. Natl. Acad. Sci. U. S. A.* **2014**, *111*, 18448. (e) McNeill, S. M.; Preston, D.; Lewis, J. E. M.; Robert, A.; Knerr-Rupp, K.; Graham, D. O.; Wright, J. R.; Giles, G. I.; Crowley, J. D. *Dalton Trans.* **2015**, *44*, 11129.
- (2) (a) Kang, J.; Santamaria, J.; Hilmersson, G.; Rebek, J. *J. Am. Chem. Soc.* **1998**, *120*, 7389. (b) Merlau, M. L.; Mejia, M. d. P.; Nguyen, S. T.; Hupp, J. T. *Angew. Chem., Int. Ed.* **2001**, *40*, 4239. (c) Slagt, V. F.; Reek, J. N. H.; Kamer, P. C. J.; van Leeuwen, P. W. N. M. *Angew. Chem., Int. Ed.* **2001**, *40*, 4271. (d) Yoshizawa, M.; Tamura, M.; Fujita, *Science* **2006**, *312*, 251. (e) Pluth, M. D.; Bergman, R. G.; Raymond, K. N. *Science* **2007**, *316*, 85. (f) Yoon, H. J.; Kuwabara, J.; Kim, J.-H.; Mirkin, C. A. *Science* **2010**, *330*, 66. (g) Hastings, C. J.; Pluth, M. D.; Bergman, R. G.; Raymond, K. N. *J. Am. Chem. Soc.* **2010**, *132*, 6938. (h) Salles, A. G.; Zarra, S.; Turner, R. M.; Nitschke, J. R. *J. Am. Chem. Soc.* **2013**, *135*, 19143. (i) Kaphan, D. M.; Levin, M. D.; Bergman, R. G.; Raymond, K. N.; Toste, F. D. *Science* **2015**, *350*, 1235. (j) Cullen, W.; Misuraca, M. C.; Hunter, C. A.; Williams, N. H.; Ward, M. D. *Nat. Chem.* **2016**, *8*, 231. (k) Wang, Q.-Q.; Gonell, S.; Leenders, S. H. A. M.; Dürr, M.; Ivanović-Burmazović, I.; Reek, J. N. H. *Nat. Chem.* **2016**, *8*, 225.
- (3) (a) Yoshizawa, M.; Kusukawa, T.; Fujita, M.; Yamaguchi, K. *J. Am. Chem. Soc.* **2000**, *122*, 6311. (b) Mal, P.; Breiner, B.; Rissanen, K.; Nitschke, J. R. *Science* **2009**, *324*, 1697. (c) Liu, Y.; Hu, C.; Comotti, A.; Ward, M. D. *Science* **2011**, *333*, 436.
- (4) While the vast majority of self-assembly reactions are under overall (reversible) thermodynamic control, some often display significant levels of cooperativity that direct the self-assembly reaction down a particular (kinetic) pathway. The hallmark of a kinetically controlled self-assembly reaction is often the sensitivity to the sequence of addition of components. For a very elegant example of this, see: Levin, M. D.; Stang, P. J. *J. Am. Chem. Soc.* **2000**, *122*, 7428.
- (5) (a) Dalgarno, S. J.; Power, N. P.; Atwood, J. L. *Coord. Chem. Rev.* **2008**, *252*, 825. (b) Chakrabarty, R.; Mukherjee, P. S.; Stang, P. J. *Chem. Rev.* **2011**, *111*, 6810. (c) Mukherjee, S.; Mukherjee, P. S. *Chem. Commun.* **2014**, *50*, 2239. (d) Cook, T. R.; Stang, P. J. *Chem. Rev.* **2015**, *115*, 7001.
- (6) (a) Fujita, M.; Sasaki, O.; Mitsuhashi, T.; Fujita, T.; Yazaki, J.; Yamaguchi, K.; Ogura, K. *Chem. Commun.* **1996**, 1535. (b) Schweiger, M.; Seidel, S. R.; Arif, A. M.; Stang, P. J. *Inorg. Chem.* **2002**, *41*, 2556. (c) Cotton, F. A.; Murillo, C. A.; Yu, R. *Dalton Trans.* **2006**, 3900.
- (7) Riddell, I. A.; Ronson, T. K.; Clegg, J. K.; Wood, C. S.; Bilbeisi, R. A.; Nitschke, J. R. *J. Am. Chem. Soc.* **2014**, *136*, 9491.
- (8) (a) Hunter, C. A.; Anderson, H. L. *Angew. Chem., Int. Ed.* **2009**, *48*, 7488. For example of chelate cooperativity in coordination assemblies, see: (b) Sato, S.; Ishido, Y.; Fujita, M. *J. Am. Chem. Soc.* **2009**, *131*, 6064. (c) Henkelis, J. J.; Fisher, J.; Warriner, S. L.; Hardie, M. J. *Chem. - Eur. J.* **2014**, *20*, 4117.
- (9) Thomas, J. A. *Chem. Soc. Rev.* **2007**, *36*, 856.
- (10) For reviews on DCC, see: (a) Corbett, P. T.; Leclair, J.; Vial, L.; West, K. R.; Wietor, J.-L.; Sanders, J. K. M.; Otto, S. *Chem. Rev.*

2006, 106, 3652. (b) Jin, Y.; Yu, C.; Denman, R. J.; Zhang, W. *Chem. Soc. Rev.* **2013**, 42, 6634.

(11) (a) Hamilton, D. G.; Feeder, N.; Teat, S. J.; Sanders, J. K. M. *New J. Chem.* **1998**, 22, 1019. (b) Kidd, T. J.; Leigh, D. A.; Wilson, A. J. *J. Am. Chem. Soc.* **1999**, 121, 1599. (c) Glink, P. T.; Oliva, A. I.; Stoddart, J. F.; White, A. J. P.; Williams, D. J. *Angew. Chem., Int. Ed.* **2001**, 40, 1870. (d) Kilbinger, A. F. M.; Cantrill, S. J.; Waltman, A. W.; Day, M. W.; Grubbs, R. H. *Angew. Chem., Int. Ed.* **2003**, 42, 3281. (e) Hogg, L.; Leigh, D. A.; Lusby, P. J.; Morelli, A.; Parsons, S.; Wong, J. K. Y. *Angew. Chem., Int. Ed.* **2004**, 43, 1218. (f) Peters, A. J.; Chichak, K. S.; Cantrill, S. J.; Stoddart, J. F. *Chem. Commun.* **2005**, 3394. (g) Lam, R. T. S.; Belenguer, A.; Roberts, S. L.; Naumann, C.; Jarrosson, T.; Otto, S.; Sanders, J. K. M. *Science* **2005**, 308, 667. (h) West, K. R.; Ludlow, R. F.; Corbett, P. T.; Besenius, P.; Mansfield, F. M.; Cormack, P. A. G.; Sherrington, D. C.; Goodman, J. M.; Stuart, M. C. A.; Otto, S. *J. Am. Chem. Soc.* **2008**, 130, 10834. (i) Wood, C. S.; Ronson, T. K.; Belenguer, A. M.; Holstein, J. J.; Nitschke, J. R. *Nat. Chem.* **2015**, 7, 354.

(12) (a) Liu, X.; Liu, Y.; Li, G.; Warmuth, R. *Angew. Chem., Int. Ed.* **2006**, 45, 901. (b) Christinat, N.; Scopelliti, R.; Severin, K. *Angew. Chem., Int. Ed.* **2008**, 47, 1848. (c) Hiraoka, S.; Yamauchi, Y.; Arakane, R.; Shionoya, M. *J. Am. Chem. Soc.* **2009**, 131, 11646. (d) Swamy, S. I.; Bacsá, J.; Jones, J. T. A.; Stylianou, K. C.; Steiner, A.; Ritchie, L. K.; Hasell, T.; Gould, J. A.; Laybourn, A.; Khimiyak, Y. Z.; Adams, D. J.; Rosseinsky, M. J.; Cooper, A. I. *J. Am. Chem. Soc.* **2010**, 132, 12773. (e) Zhang, C.; Wang, Q.; Long, H.; Zhang, W. *J. Am. Chem. Soc.* **2011**, 133, 20995. (f) Asadi, A.; Ajami, D.; Rebeck, J. *Chem. Sci.* **2013**, 4, 1212. (g) Mosquera, J.; Zarra, S.; Nitschke, J. R. *Angew. Chem., Int. Ed.* **2014**, 53, 1556.

(13) (a) von Delius, M.; Geertsema, E. M.; Leigh, D. A. *Nat. Chem.* **2010**, 2, 96. (b) Kovaříček, P.; Lehn, J.-M. *Chem. - Eur. J.* **2015**, 21, 9380. (c) Kassem, S.; Lee, A. T. L.; Leigh, D. A.; Markevicius, A.; Solà, J. *Nat. Chem.* **2016**, 3, 138.

(14) (a) Davis, A. V.; Raymond, K. N. *J. Am. Chem. Soc.* **2005**, 127, 7912. (b) Cangelosi, V. M.; Carter, T. G.; Zakharov, L. N.; Johnson, D. W. *Chem. Commun.* **2009**, 5606.

(15) For examples which rely on the high-temperature labilization of second- and third-row transition-metal ion–ligand interactions, see: (a) Fujita, M.; Ibukuro, F.; Hagihara, H.; Ogura, K. *Nature* **1994**, 367, 720. (b) Fujita, M.; Ibukuro, F.; Yamaguchi, K.; Ogura, K. *J. Am. Chem. Soc.* **1995**, 117, 4175. (c) Ibukuro, F.; Kusukawa, T.; Fujita, M. *J. Am. Chem. Soc.* **1998**, 120, 8561. (d) Roche, S.; Haslam, C.; Heath, S. L.; Thomas, J. A. *Chem. Commun.* **1998**, 1681. (e) Glasson, C. R. K.; Meehan, G. V.; Clegg, J. K.; Lindoy, L. F.; Smith, J. A.; Keene, F. R.; Motti, C. *Chem. - Eur. J.* **2008**, 14, 10535. For examples which utilize a combination of fixed and labile metal–ligand interactions, see: (f) Newkome, G. R.; Wang, P.; Moorefield, C. N.; Cho, T. J.; Mohapatra, P. P.; Li, S.; Hwang, S.-H.; Lukoyanova, O.; Echegoyen, L.; Palagallo, J. A.; Iancu, V.; Hla, S.-W. *Science* **2006**, 312, 1782. (g) Chepelin, O.; Ujma, J.; Barran, P. E.; Lusby, P. J. *Angew. Chem., Int. Ed.* **2012**, 51, 4194. (h) Metherell, A. J.; Ward, M. D. *Chem. Sci.* **2016**, 7, 910. Appropriate “spectator” ligands can dramatically labilize exchangeable second- and third-row M–L interactions, permitting self-assembly under ambient conditions; see: (i) Leininger, S.; Fan, J.; Schmitz, M.; Stang, P. J. *Proc. Natl. Acad. Sci. U. S. A.* **2000**, 97, 1380. (j) Chepelin, O.; Ujma, J.; Wu, X.; Slawin, A. M. Z.; Pitak, M. B.; Coles, S. J.; Michel, J.; Jones, A. C.; Barran, P. E.; Lusby, P. J. *J. Am. Chem. Soc.* **2012**, 134, 19334.

(16) Tashiro, S.; Tominaga, M.; Kusukawa, T.; Kawano, M.; Sakamoto, S.; Yamaguchi, K.; Fujita, M. *Angew. Chem., Int. Ed.* **2003**, 42, 3267.

(17) Fujita, D.; Takahashi, A.; Sato, S.; Fujita, M. *J. Am. Chem. Soc.* **2011**, 133, 13317.

(18) (a) Yamashita, K.; Kawano, M.; Fujita, M. *J. Am. Chem. Soc.* **2007**, 129, 1850. (b) Yamashita, K.; Sato, K.; Kawano, M.; Fujita, M. *New J. Chem.* **2009**, 33, 264.

(19) Symmers, P. R.; Burke, M. J.; August, D. P.; Thomson, P. I. T.; Nichol, G. S.; Warren, M. R.; Campbell, C. J.; Lusby, P. J. *Chem. Sci.* **2015**, 6, 756.

(20) (a) Charbonniere, L. J.; Bernardinelli, G.; Piguet, C.; Sargeson, A. M.; Williams, A. F. *J. Chem. Soc., Chem. Commun.* **1994**, 1419. (b) Leigh, D. A.; Lusby, P. J.; McBurney, R. T.; Morelli, A.; Slawin, A. M. Z.; Thomson, A. R.; Walker, D. B. *J. Am. Chem. Soc.* **2009**, 131, 3762. (c) Mugemana, C.; Guillet, P.; Hoepfener, S.; Schubert, U. S.; Fustin, C.-A.; Gohy, J.-F. *Chem. Commun.* **2010**, 46, 1296. (d) Constable, E. C.; Harris, K.; Housecroft, C. E.; Neuburger, M. *Dalton Trans.* **2011**, 40, 1524. (e) Ayme, J.-F.; Lux, J.; Sauvage, J.-P.; Sour, A. *Chem. - Eur. J.* **2012**, 18, 5565. For a similar use of Cr^{II}/Cr^{III}, see: (f) Cantuel, M.; Bernardinelli, G.; Imbert, D.; Bünzli, J.-C. G.; Hopfgartner, G.; Piguet, C. *J. Chem. Soc., Dalton Trans.* **2002**, 1929.

(21) With rigid, bis(bidentate) ligands and metal ions with strong octahedral preference, M₂L₃ helicates are generally observed only as minor equilibrium components; see: (a) Glasson, C. R. K.; Meehan, G. V.; Motti, C. A.; Clegg, J. K.; Turner, P.; Jensen, P.; Lindoy, L. F. *Dalton Trans.* **2011**, 40, 10481. (b) Ousaka, N.; Grunder, S.; Castilla, A. M.; Whalley, A. C.; Stoddart, J. F.; Nitschke, J. R. *J. Am. Chem. Soc.* **2012**, 134, 15528. With non-labile octahedral metal ions, e.g., Ru^{II}, M₂L₃ helicates can be obtained in low yields using rigid ligands, suggesting these are kinetically trapped intermediates (see ref 15e).

(22) (a) Hernandez, J. V.; Kay, E. R.; Leigh, D. A. *Science* **2004**, 306, 1532. (b) Cheng, C.; McGonigal, P. R.; Liu, W.-G.; Li, H.; Vermeulen, N. A.; Ke, C.; Frascioni, M.; Stern, C. L.; Goddard, W. A., III; Stoddart, J. F. *J. Am. Chem. Soc.* **2014**, 136, 14702. (c) Ragazzon, G.; Baroncini, M.; Silvi, S.; Venturi, M.; Credi, A. *Nat. Nanotechnol.* **2015**, 10, 70.

(23) (a) Scherer, M.; Caulder, D. L.; Johnson, D. W.; Raymond, K. N. *Angew. Chem., Int. Ed.* **1999**, 38, 1587. (b) Xu, J.; Parac, T. N.; Raymond, K. N. *Angew. Chem., Int. Ed.* **1999**, 38, 2878. (c) Beissel, T.; Powers, R. E.; Parac, T. N.; Raymond, K. N. *J. Am. Chem. Soc.* **1999**, 121, 4200. (d) Stephenson, A.; Argent, S. P.; Riis-Johannessen, T.; Tidmarsh, I. S.; Ward, M. D. *J. Am. Chem. Soc.* **2011**, 133, 858. (e) Riddell, I. A.; Smulders, M. M. J.; Clegg, J. K.; Hristova, Y. R.; Breiner, B.; Thoburn, J. D.; Nitschke, J. R. *Nat. Chem.* **2012**, 4, 751. (f) Zarra, S.; Clegg, J. K.; Nitschke, J. R. *Angew. Chem., Int. Ed.* **2013**, 52, 4837. (g) Meng, W.; Ronson, T. K.; Clegg, J. K.; Nitschke, J. R. *Angew. Chem., Int. Ed.* **2013**, 52, 1017. (h) Young, M. C.; Johnson, A. M.; Gamboa, A. S.; Hooley, R. J. *Chem. Commun.* **2013**, 49, 1627. (i) Young, M. C.; Holloway, L. R.; Johnson, A. M.; Hooley, R. J. *Angew. Chem., Int. Ed.* **2014**, 53, 9832. (j) Cullen, W.; Hunter, C. A.; Ward, M. D. *Inorg. Chem.* **2015**, 54, 2626.

(24) \sum , the sum of the absolute deviations from 90° of the 12 cis angles, is averaged at 45° for 2c and 41° for 2d. The twist angles are $\theta = 55^\circ$ (2c) and 54° (2d) [0° = ideal trigonal prismatic; 60° = ideal octahedral].

(25) (a) Seeber, G.; Tiedemann, B. E. F.; Raymond, K. N. *Top. Curr. Chem.* **2006**, 265, 147. (b) Castilla, A. M.; Ramsay, W. J.; Nitschke, J. R. *Chem. Lett.* **2014**, 43, 256.

(26) (a) Fujita, N.; Biradha, K.; Fujita, M.; Sakamoto, S.; Yamaguchi, K. *Angew. Chem., Int. Ed.* **2001**, 40, 1718. (b) Hiraoka, S.; Harano, K.; Shiro, M.; Shionoya, M. *Angew. Chem., Int. Ed.* **2005**, 44, 2727. (c) Hiraoka, S.; Sakata, Y.; Shionoya, M. *J. Am. Chem. Soc.* **2008**, 130, 10058. (d) Zhao, L.; Northrop, B. H.; Stang, P. J. *J. Am. Chem. Soc.* **2008**, 130, 11886. (e) Oliveri, C. G.; Ulmann, P. A.; Wiester, M. J.; Mirkin, C. A. *Acc. Chem. Res.* **2008**, 41, 1618. (f) Aimi, J.; Nagamine, Y.; Tsuda, A.; Muranaka, A.; Uchiyama, M.; Aida, T. *Angew. Chem., Int. Ed.* **2008**, 47, 5153. (g) Kilbas, B.; Mirtschin, S.; Scopelliti, R.; Severin, K. *Chem. Sci.* **2012**, 3, 701–704. (h) Yi, S.; Brega, V.; Captain, B.; Kaifer, A. E. *Chem. Commun.* **2012**, 48, 10295. (i) Neogi, S.; Lorenz, Y.; Engeser, M.; Samanta, D.; Schmittel, M. *Inorg. Chem.* **2013**, 52, 6975. (j) Stadler, A.-M.; Burg, C.; Ramírez, J.; Lehn, J.-M. *Chem. Commun.* **2013**, 49, 5733. (k) Lu, X.; Li, X.; Guo, K.; Xie, T.-Z.; Moorefield, C. N.; Wesdemiotis, C.; Newkome, G. R. *J. Am. Chem. Soc.* **2014**, 136, 18149. (l) Zhu, R.; Luebben, J.; Dittrich, B.; Clever, G. H. *Angew. Chem., Int. Ed.* **2015**, 54, 2796. (m) Jurček, O.; Bonakdarzadeh, P.; Kalenius, E.; Linnanto, J. M.; Groessl, M.; Knochenmuss, R.; Ihalainen, J. A.; Rissanen, K. *Angew. Chem., Int. Ed.* **2015**, 54, 15462. (n) Preston, D.; Fox-Charles, A.; Lo, W. K. C.; Crowley, J. D. *Chem. Commun.* **2015**, 51, 9042. (o) Han, M.; Luo, Y.; Damaschke, B.; Gomez, L.; Ribas, X.; Jose, A.; Peretzki, P.; Seibt, M.; Clever, G. H.

Angew. Chem., Int. Ed. **2016**, *55*, 445. For a recent redox-induced metallosupramolecular disassembly reassembly process, see: (p) Croué, V.; Goeb, S.; Szalóki, G.; Allain, M.; Sallé, M. *Angew. Chem., Int. Ed.* **2016**, *55*, 1746.

(27) (a) Nicewicz, D. A.; MacMillan, D. W. C. *Science* **2008**, *322*, 77. (b) Narayanam, J. M. R.; Stephenson, C. R. J. *Chem. Soc. Rev.* **2011**, *40*, 102. For an early example of photoredox catalysis using inexpensive Cu phenanthroline complexes, see: (c) Kern, J.-M.; Sauvage, J.-P. *J. Chem. Soc., Chem. Commun.* **1987**, 546.

(28) (a) Tanner, M. E.; Knobler, C. B.; Cram, D. J. *J. Am. Chem. Soc.* **1990**, *112*, 1659. (b) Kang, B.; Kurutz, J. W.; Youm, K.-T.; Totten, R. K.; Hupp, J. T.; Nguyen, S. T. *Chem. Sci.* **2012**, *3*, 1938. (c) Liu, S.; Russell, D. H.; Zinnel, N. F.; Gibb, B. C. *J. Am. Chem. Soc.* **2013**, *135*, 4314. (d) Dale, E. J.; Vermeulen, N. A.; Thomas, A. A.; Barnes, J. C.; Juricek, M.; Blackburn, A. K.; Strutt, N. L.; Sarjeant, A. A.; Stern, C. L.; Denmark, S. E.; Stoddart, J. F. *J. Am. Chem. Soc.* **2014**, *136*, 10669.

(29) Karnthaler-Benbakka, C.; Groza, D.; Kryeziu, K.; Pichler, V.; Roller, A.; Berger, W.; Heffeter, P.; Kowol, C. R. *Angew. Chem., Int. Ed.* **2014**, *53*, 12930.